CRREL

12

CRREL

Ice arching and the drift of pack ice through restricted channels

DDC
SEP 19 1977

AD A044218

AD No.
DDC FILE COPY

For conversion of SI metric units to U.S./British customary units of measurement consult ASTM Standard E380, Metric Practice Guide, *published by the American Society for Testing and Materials, 1916 Race St., Philadelphia, Pa. 19103.*

Cover: LANDSAT imagery of ice drift through Bering Strait, March 1973.

CRREL Report 77-18

Ice arching and the drift of pack ice through restricted channels

D.S. Sodhi

August 1977

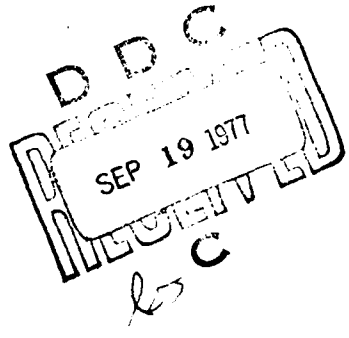

Prepared for
BUREAU OF LAND MANAGEMENT
By
CORPS OF ENGINEERS, U.S. ARMY
COLD REGIONS RESEARCH AND ENGINEERING LABORATORY
HANOVER, NEW HAMPSHIRE

Approved for public release, distribution unlimited.

Unclassified

SECURITY CLASSIFICATION OF THIS PAGE (When Date Entered)

REPORT DOCUMENTATION PAGE

READ INSTRUCTIONS BEFORE COMPLETING FORM

1. REPORT NUMBER: CRREL [redacted] 77-18
2. GOVT ACCESSION NO.
3. RECIPIENT'S CATALOG NUMBER

4. TITLE (and Subtitle): ICE ARCHING AND THE DRIFT OF PACK ICE THROUGH RESTRICTED CHANNELS
5. TYPE OF REPORT & PERIOD COVERED
6. PERFORMING ORG. REPORT NUMBER

7. AUTHOR(s): [redacted] S. Sodhi
8. CONTRACT OR GRANT NUMBER(s): NOAA/BLM Research Unit 88; NRC Research Grant A867

9. PERFORMING ORGANIZATION NAME AND ADDRESS: U.S. Army Cold Regions Research and Engineering Laboratory, Hanover, New Hampshire 03755
10. PROGRAM ELEMENT, PROJECT, TASK AREA & WORK UNIT NUMBERS

11. CONTROLLING OFFICE NAME AND ADDRESS: Bureau of Land Management, Washington, D.C.
12. REPORT DATE: Aug[redacted] 77
13. NUMBER OF PAGES: 171

14. MONITORING AGENCY NAME & ADDRESS (if different from Controlling Office): National Oceanic and Atmospheric Administration, Boulder, Colorado
15. SECURITY CLASS. (of this report): Unclassified
15a. DECLASSIFICATION/DOWNGRADING SCHEDULE

16. DISTRIBUTION STATEMENT (of this Report)

Approved for public release; distribution unlimited.

17. DISTRIBUTION STATEMENT (of the abstract entered in Block 20, if different from Report)

Partial funding provided by the National Research Council of Canada.

18. SUPPLEMENTARY NOTES

19. KEY WORDS (Continue on reverse side if necessary and identify by block number)

Arching
Channels
Drift
Ice
Mathematical models
Sea ice

20. ABSTRACT (Continue on reverse side if necessary and identify by block number)

Models originally developed to describe the arching and the movement of granular materials through hoppers or chutes are applied to the arching and drift of pack ice in straits and gulfs having lengths of 50 to 500 km. Verification of the usefulness of the models is attempted by making comparisons with ice deformation patterns as observed via satellite imagery in the Bering Strait region and in Amundsen Gulf. The results are encouraging in that there is good correspondence between observed arching and lead patterns and those predicted by theory. In addition, values determined via the model for the angle of internal friction ($\approx 30^{\circ}$ to 35°) and the cohesive strength per unit thickness ($\approx$ 2000 N/m) are similar to values obtained by other approaches. It is estimated that if the wind velocity parallel to the Bering Strait exceeds $\approx$ 6 m/s, there will be ice flow through the strait.

DD FORM 1 JAN 73 1473 EDITION OF 1 NOV 65 IS OBSOLETE

Unclassified

SECURITY CLASSIFICATION OF THIS PAGE (When Date Entered)

PREFACE

The report was prepared by Dr. Devinder S. Sodhi, Associate Professor, Memorial University of Newfoundland, during a period of time when he was a visiting scientist at CRREL. The study was primarily supported as a part of Research Unit 88, *Dynamics of Near-Shore Ice* by the Bureau of Land Management through interagency agreement with the National Oceanic and Atmospheric Administration. It is part of a multiyear program responding to the needs of petroleum development of the Alaskan continental shelf managed by the Outer Continental Shelf Environmental Assessment Program. Funding was also provided by the National Research Council of Canada under Research Grant A867.

Dr. W.F. Weeks and Stephen F. Ackley of CRREL technically reviewed this report.

The author would like to thank Dr. Weeks for valuable suggestions during the writing of this paper and for providing the DMSP imagery. Appreciation is also expressed to Austin Kovacs for providing valuable suggestions and information.

CONTENTS

	Page
Abstract	i
Preface	ii
Introduction	1
Theory	1
Limiting span of an arch	2
Flow of pack ice through converging channels	3
Stoppage of flow	3
Applications	4
St. Lawrence Island	4
Amundsen Gulf	5
Bering Strait	5
Conclusion	10
References	10

ILLUSTRATIONS

Figure	
1. Free arch	2
2. Mohr circle	2
3. Effective yield locus in Jenike's model	3
4. Converging channel	4
5. LANDSAT imagery showing wedge-shaped ice accumulation north of St. Lawrence Island, 24 February 1975	4
6. LANDSAT imagery of an arch across Amundsen Gulf, 12 June 1973	6
7. LANDSAT imagery of breakup of an arch across Amundsen Gulf, 13 June 1973	7
8. DMSP imagery of the ice drift through Bering Strait, 20 January 1976	8
9. DMSP imagery of the ice drift through Bering Strait, 6 February 1976	8
10. Ice drift through Bering Strait, 7 March 1973	9
11. DMSP imagery showing crack pattern due to shearing, Bering Strait, 8 December 1975	10

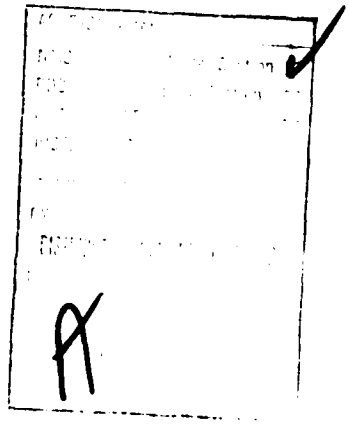

ICE ARCHING AND THE DRIFT OF PACK ICE THROUGH RESTRICTED CHANNELS

D.S. Sodhi

INTRODUCTION

In this report the factors influencing ice arching across straits or gulfs are investigated by developing an analogy between the drift of pack ice through a restricted channel between converging land masses and the gravity flow of granular material through hoppers or chutes. This approach appears reasonable because of the similarity of the basic mechanics of the two situations, pack ice being composed of interacting ice floes that transfer stresses across their boundaries in a manner that is presumably similar to the force interaction between grains of a granular material. Also supporting the applicability of such an approach is the knowledge that Janssen's (1895) theory for the flow of grain in a silo has been used (Pariset and Hauser 1961, Michel 1968) to calculate, for fragmented ice covers moving through straight river channels, forces that were in reasonable agreement with experimental observations.

Other work of interest is by Shapiro and Burns (1975) who described, via the use of LANDSAT imagery, a short-term episode (6–8 March 1973) of the rapid deformation of pack ice in the southeastern Chukchi Sea and its subsequent transport south through the Bering Strait. They suggested that the process of ice passing through the strait is mechanically similar to the extrusion of metal through a restricted orifice. They did not, however, attempt to use extrusion flow theory to make detailed calculations concerning the behavior of pack ice. We believe that granular media models have advantages here, inasmuch as pack ice is a granular medium both before and after passing through a strait while a metal is invariably continuous after passing through a die. Also, the principal force which drives the ice, the force of the wind, can be considered more analogous to the specific weight of a granular material than to the forces involved in extrusion.

A kinematic model study of the arching phenomena in drifting ice was undertakn by Calkins and Ashton (1975) who performed experiments in a flume using square plastic pieces to simulate ice floes. The plastic floes were released at a controlled rate upstream from a channel restriction and the occurrence or nonoccurrence of a stable arch was noted. Good correlations were obtained between the threshold of arching and parameters such as the supply rate of the surface area of ice, the surface discharge at the gap, and the ratio between the size of the individual floes and the size of the gap. Because their interests were directed toward ice jams in rivers, Calkins and Ashton (1975) did not study the case when the ratio of the floe size to the gap dimension is small, the subject of interest here.

In this report a theory will be developed and then applied to ice arching in the Bering Strait and Amundsen Gulf via an analysis of the geometry of the arching phenomena as revealed by satellite imagery. This analysis allows one to calculate representative values for the angle of internal friction and the cohesive strength of pack ice as viewed on a large scale. In addition, comparisons are made between the lead patterns as revealed by the satellite imagery and faults (tangential velocity discontinuities) that are determined by a radial stress field solution of the basic equations.

THEORY

An essential requirement of the various theories for the flow of granular material is that they obey Coulomb's yield criterion. One group of theories (Drucker and Prager 1952) is based on the assumptions that 1) the Mohr–Coulomb yield function is the plastic potential for the material, so that the strain rate components are related to the yield function by the associated flow rate of plasticity, and that 2) the principal axes of the stress

and strain rate tensors coincide. An inevitable consequence of these postulates is that there is an unrealistic volume expansion during deformation. In an attempt to overcome this difficulty, work hardening models have been proposed by Drucker et al. (1957), Jenike and Shield (1959), and Jenike (1961). In these models, cohesion is a function of the density of the material as well as the hydrostatic pressure to which it is subjected. Another group of theories (de Josselin de Jong 1959, Spencer 1964, Mandl and Lugue 1970) has sought to retain volume constancy, thus abandoning the concept of normality and the coincidence of the principal axes of the stress and strain rate tensors. Of these latter theories, that of Spencer (1964) appears to be the most satisfactory, particularly since it allows faults on the Coulomb surfaces, and has recently been extended to include gravitational and inertial acceleration terms (Morrison and Richmond 1976).

No matter which theory is followed, one ends up with a set of hyperbolic differential equations which can be solved by the method of characteristics (slip line fields), provided the boundary conditions are well-defined. Simplifying assumptions commonly have to be made to arrive at simple solutions and a number of such solutions exist in the literature (Walker 1966, Johanson and Jenike 1967, Lee 1973).

In this report, we would like to pay attention to three aspects of the problem: 1) the limiting span of an arch that has formed across a strait, 2) the flow of pack ice through converging channels, and 3) the critical condition of stoppage of such a flow. The theories dealing with each aspect of the problem are discussed briefly below.

Limiting span of an arch

The theory for predicting the limiting spans for the arching of granular material is based on a static analysis of the stress distribution within the material to ascertain whether the state of stress is always below the critical state. To derive expressions determining the upper and lower boundaries for the limiting span over which a free arch can form, we will follow the analysis given by Richmond and Gardner (1962) and Gardner (1962) by making the following modifying assumptions:

1. In the vicinity of a free arch the stress is invariate with respect to the longitudinal coordinate. This assumption has been verified by many investigators in deep vertical grain silos and by Michel (1968, 1971) in long straight channels full of fragmented ice.

2. The material can be approximated as a continuum which obeys Coulomb's failure criterion.

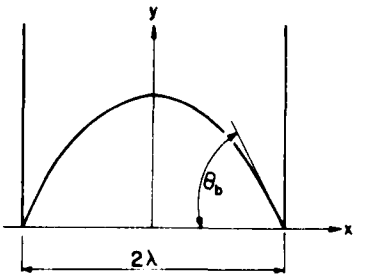

Figure 1. Free arch.

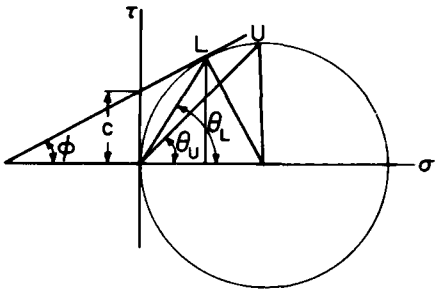

Figure 2. Mohr circle.

3. The failure criterion holding at the boundary between the granular material and its container (i.e. between the pack ice and the "containing" fast ice) is the same as within the material.

In the following, the upper boundary will be defined as the maximum span across which an arch can possibly form with the state of stress at all points still remaining below the critical level. The lower boundary, on the other hand, is the minimum span through which flow can still occur.

To develop the conditions requisite for free arching, we will choose the Cartesian coordinate system shown in Figure 1. Making use of assumption 1, the equilibrium equations can be satisfied by the following expressions for the normal and shear stress components σ_x and τ_{xy}:

$$\sigma_x = -p \tag{1}$$

and

$$\tau_{xy} = \gamma x \tag{2}$$

where p is a constant and γ is the body force per unit area. The state of stress at a point on the free arch can be conveniently expressed with the help of a Mohr

circle (Fig. 2) which must pass through the origin of the (τ, σ) graph. Coulomb's failure criterion is expressed by a yield line:

$$\tau = c + \sigma \tan\phi \tag{3}$$

where c and ϕ are the cohesive strength and angle of internal friction, respectively. If the Mohr stress circle is tangent to the yield line, the state of stress is critical. According to eq 2, the maximum shear stress occurs at the boundary, and we can express the upper and lower bounds by points U and L in Figure 2 by incorporating assumptions 2 and 3. The limiting values of the span are given by the following expressions (Richmond and Gardner 1962):

$$\lambda_U = \frac{c}{\gamma} \frac{\cos\phi}{(1 - \sin\phi)} \tag{4}$$

and

$$\lambda_L = \frac{c}{\gamma} (1 + \sin\phi) . \tag{5}$$

The shape of the limiting arch can be obtained with the aid of the stress circle shown in Figure 2. If θ is the angle between the horizontal and the tangent to the free surface, the arch profile is given by

$$\tan\theta = -\frac{dy}{dx} = -\frac{\tau_{xy}}{\sigma_x} = \frac{\gamma x}{p} . \tag{6}$$

Integrating and assuming $y = 0$ when $x = \lambda$, we obtain

$$y = \frac{\gamma\lambda^2}{2p} \left[1 - \left(\frac{x}{\lambda}\right)^2\right] \tag{7}$$

indicating that the profile of the limiting arch should be a parabola.

The angle θ_b in Figure 1 will either be equal to θ_U or θ_L in Figure 2, depending upon whether the arch is of the upper or lower boundary type. θ_U is equal to 45° and θ_L can be shown, with the help of the stress circle in Figure 2, to be equal to $\pi/4 + \phi/2$. The base angle θ_b can therefore be used to estimate the angle of internal friction ϕ.

Flow of pack ice through converging channels

When ice is moving through a restricted channel, Jenike's (1964) model of the steady gravity flow of granular material through a converging channel can be used to obtain the locations at which velocity discontinuities (i.e. cracks or leads) will occur. In this

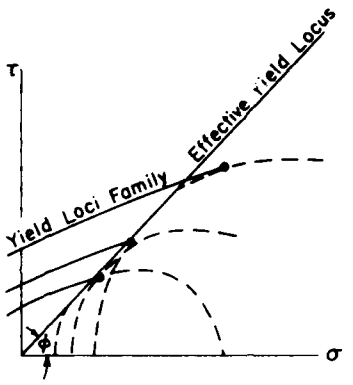

Figure 3. Effective yield locus in Jenike's (1964) model.

model there is assumed to exist a family of similar but varying yield loci corresponding to different degrees of consolidation. Each locus terminates at the stress appropriate to its consolidation (i.e. the material cannot be subjected to a higher stress without becoming further consolidated). The envelope of terminal Mohr circles of individual yield loci that is termed the "effective yield locus" (Fig. 3) represents the shear-compressive stress characteristic of the material. For many granular materials, the effective yield locus is linear and passes through the origin (Jenike 1961); therefore, we will also assume that this is true for the case of pack ice. When the state of stress is such that the Mohr circle is tangent to the effective yield locus, the material is said to be in a critical state, i.e. steady state of flow. According to this theory, one obtains two separate sets of stress and velocity characteristics, and any velocity discontinuity will be along the velocity characteristics. In the application considered later, we will use the radial stress field solution proposed by Jenike (1964), which is valid near the outlet of the converging channel, and assume that the hydrostatic stress is proportional to the distance from the vertex of the channel.

Stoppage of flow

The most complete analysis of the non-steady flow of granular material in a converging channel is by Morrison and Richmond (1976). It uses the ideal soil model proposed by Spencer (1964), which is based on the assumptions of material isotropy and incompressibility together with the postulate that deformation occurs by shear along the characteristic curves of the stress equations. This model is particularly satisfactory for the present application because it allows tangential velocity discontinuities (faults) along the stress

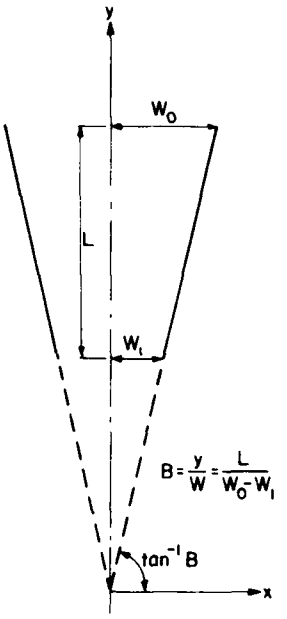

Figure 4. Converging channel.

characteristics. Based on Morrison and Richmond's (1976) analysis, the critical value of the slope B of a converging channel (see Fig. 4) for which no flow or arching may occur is given by

$$B_c = \frac{c \cot\phi\,(1 - 3\sin\phi)}{(\rho g)\, W_0\,(1 - \sin\phi)} \left(\frac{R^m - 1}{1 - R^{m-1}}\right) \qquad (8)$$

where B_c = critical value of the slope of the channel
c = cohesive strength of the material
ϕ = angle of internal friction of the material
W_0, W_1 = half widths of channel at entry and at exit, respectively
$R = W_0/W_1$
(ρg) = specific weight of the material
$m = (2 \sin\phi)/(1 - \sin\phi)$.

If $B < B_c$ arching will occur.

APPLICATIONS

St. Lawrence Island

This island is situated directly south of the Bering Strait. As the ice drifts southward through the strait and moves past the island, there is a wedge-shaped accumulation of ice that builds up on the north side of the island, as shown in Figure 5. This phenomenon is similar to the piling of granular material on an obstruction placed in the flow of granular material.

Figure 5. LANDSAT imagery showing wedge-shaped ice accumulation north of St. Lawrence Island, 24 February 1975.

Using Spencer's (1964) soil theory, the sliding surfaces can be interpreted as the stress characteristic lines for a constant orientation of principal stresses in the pack ice, as shown in Figure 5. The smaller angle between the characteristic lines can be shown to be equal to $[(\pi/2) - \phi]$. The wedge angle in Figure 5 is approximately equal to 59°, from which we can calculate the angle of internal friction to be equal to 31°.

A similar wedge-shaped ice buildup has been noted by Dunbar and Weeks (1975) in the ice next to Prince Edward Island in the Gulf of St. Lawrence. The angle between the characteristic lines at that site was 50°, corresponding to an angle of internal friction of 40°.

Amundsen Gulf

The ice arch across Amundsen Gulf in the western Canadian Arctic (≈ 71°N, 123°W) is quite clearly shown in the LANDSAT imagery obtained on 12 and 13 June 1973 (Fig. 6 and 7). The profile of the arch is approximately parabolic, which is in agreement with the shape predicted by eq 6. Although the breakup of the arch had started on 12 June (Fig. 6), the complete collapse took place on 13 June (Fig. 7). The shearing of ice at the base of the arch is evident in Figures 6 and 7.

The angle of internal friction ϕ is obtained by measuring the angle of the arch at the base, which is equal to $2h/\lambda$ in the case of a parabola, h being the height and λ being the semi-span of the parabola. Because this angle is greater than 45°, it suggests that the arch is a limiting lower bound arch. This is, of course, in agreement with the observation that the arch had started to break up. From the imagery, the angle of the arch at the base is found to be approximately 62.5°, from which ϕ is estimated to be $2(62.5 - \pi/4) = 35°$. Now that ϕ is known, a value can be obtained for the cohesive strength c of the pack ice via eq 5 if an adequate estimate can be given of γ, the body force per unit area. In the sea ice case, γ corresponds to the resultant force on the ice primarily produced by the combination of the wind force (on the upper ice surface) and the water force (on the lower ice surface). As a first approximation we will consider the water force to be negligible and discuss only the wind force.

The closest wind observations to the area of interest were from Sachs Harbour, N.W.T., on 12 June 1973 where the maximum and mean winds were reported to be 6.25 m/s and 4.5 m/s, respectively, from the southeast to the south. The direction of the waves in the LANDSAT imagery of 12 June indicates that the wind direction was southerly. The direction of drift of ice floes, as determined from their positions on two consecutive days, suggests that the average wind direction on 13 June 1973 was southeasterly, approximately perpendicular to the base of the parabola. A rough estimate of the wind stress per unit area, which we will take to be equal to γ, can be obtained from

$$\gamma = \rho D v^2 \qquad (9)$$

where ρ is the mass density of the air, D the drag coefficient, and v the wind velocity. Using a drag coefficient of 0.001 (Hibler and Mock 1973, Banke and Smith 1973), the wind stress is estimated to be equal to 0.051 N/m^2. Now taking the span 2λ to be approximately 123 km, we can estimate from eq 5 that the cohesive strength is 1993 N/m. It is interesting to note that Pariset and Hauser (1961) estimated the cohesive strength between fragmented river ice and the river bank to be equal to a value between 1095 N/m and 1320 N/m, values which are of the same order of magnitude as we obtained.

Bering Strait

Figures 8 and 9 show infrared imagery of the Bering Strait region obtained by the U.S. Defense Meteorology Satellite Program. In these images, lighter areas indicate high temperature zones, which in this case are either open or newly refrozen leads in the pack ice. It is obvious from these images that the Bering Strait is, in fact, a converging channel similar to those treated in the chute and hopper theories. (Another view of this region is shown on the cover.)

Using the results of Jenike's radial stress field solution (Johanson and Jenike 1967), which we discussed earlier, velocity characteristics were constructed for the converging channel shown in Figure 10 and were matched with the major leads (cracks) shown in the LANDSAT imagery. A good fit was obtained when the effective angles of internal friction within both the pack ice and the stationary fast ice were chosen to be 30°.

We can use eq 8 to predict the conditions required for no flow or arching in the strait, modeled as a converging channel of slope B, by replacing the specific weight (ρg) with the applicable wind stress. If the wind stress is less than that required to produce the critical condition of flow, arching may occur. To obtain an estimate of critical wind velocity, values of B, R and W_0 are measured from Figures 8 and 9. Then using the values of c and ϕ obtained earlier, the wind velocities necessary to cause $B = B_c$ are calculated from eq 9. The relations indicate that as long as the wind velocity exceeds a value of 5.6 m/s through the Bering Strait, there will be a flow of ice through the Strait in the general manner shown in the imagery.

In some of the DMSP images of the Bering Strait region (Fig. 11), one can observe long leads in the southeastern Chukchi Sea that separate the moving pack ice from the stationary ice. One can also observe smaller leads that originate from the long leads. These are oriented in a direction perpendicular to the extensional strain in a manner similar to the orientation of crevasses in a glacier. If we assume that the pack ice deformation in Figure 11 occurring along the long leads is basically in pure shear, making these leads one of the stress characteristics, then it can be shown that the angle between the stress characteristic and the line perpendicular to the direction of extensional strain is $(\pi/4) - (\phi/2)$.

Figure 6. LANDSAT imagery of an arch across Amundsen Gulf, 12 June 1973.

Figure 7. LANDSAT imagery of breakup of an arch across Amundsen Gulf, 13 June 1973.

Figure 8. DMSP imagery of the ice drift through Bering Strait, 20 January 1976.

Figure 9. DMSP imagery of the ice drift through Bering Strait, 6 February 1976.

Figure 10. Ice drift through Bering Strait, 7 March 1973.

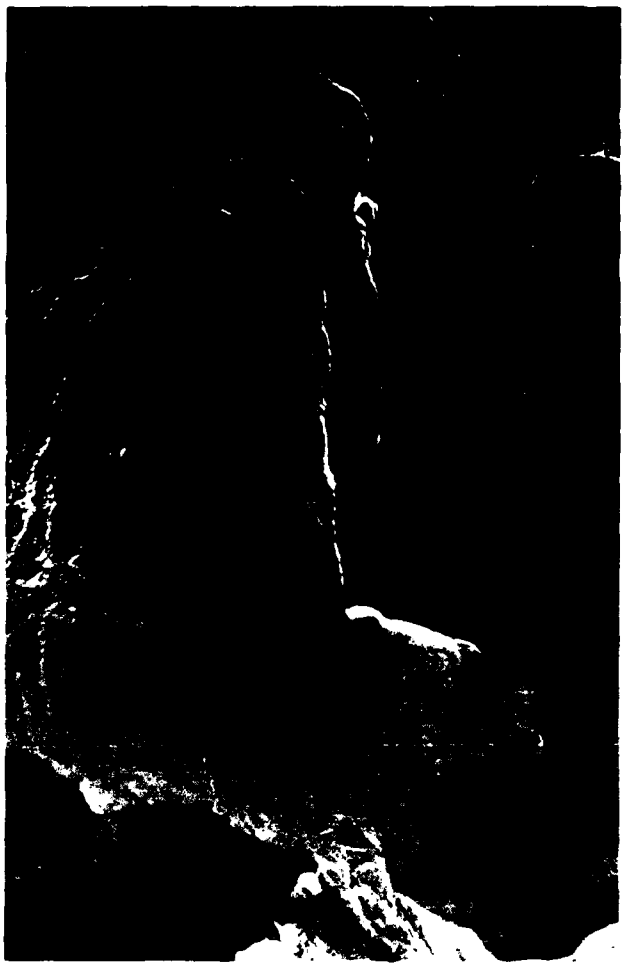

Figure 11. DMSP imagery showing crack pattern due to shearing, Bering Strait, 8 December 1975.

As measured on the DMSP imagery this angle is found to be approximately 30°, corresponding to an angle of internal friction ϕ of also 30°.

CONCLUSION

In the preceding, models originally developed to describe the arching or the movement of granular materials such as grain or sand through hoppers or chutes have been applied to the arching and drift of pack ice on a scale of 50 to 500 km. Inasmuch as experimental verification of such theories as applied to sea ice is not presently possible, comparisons are made with ice deformation patterns as observed with satellite imagery. The results of these comparisons are quite encouraging in that there is correspondence between observed arching and lead patterns and calculated patterns. Also, values determined via the model for the angle of internal friction and cohesive strength appear quite reasonable when compared with similar values available in the literature.

LITERATURE CITED

Banke, E.G. and S.D. Smith (1973) Wind stress on arctic sea ice. *Journal of Geophysical Research*, vol. 78, no. 33, p. 7871-7883.

Calkins, D.J. and G.D. Ashton (1975) Arching of fragmented ice covers. CRREL Special Report 222, AD A009499.

de Josselin de Jong, G. (1959) Statics and kinematics in the failable zone of a material. Thesis, University of Delft (unpublished).

Dunbar, M. and W.F. Weeks (1975) The interpretation of young ice forms in the Gulf of St. Lawrence using side looking airborne radar and infrared imagery. CRREL Research Report 337, AD A015457.

Drucker, D.C. and W. Prager (1952) Soil mechanics and plastic analysis or limited analysis. *Quarterly Journal of Applied Mathematics*, vol. 10, p. 157-165.

Drucker, D.C., R.E. Gibson, and D.J. Henkel (1957) Soil mechanics and work-hardening theories of plasticity. *Transactions of the American Society of Civil Engineers*, vol. 122, p. 338-346.

Gardner, G.C. (1962) Limiting conditions for flow of a cohesive granular material down an inclined plane (chute) or between parallel inclined walls (bin or channel). *Chemical Engineering Science*, vol. 17, p. 1079-1086.

Hibler, W.D. III and S.J. Mock (1973) Classification of sea ice ridging and surface roughness in the Arctic Basin. *Symposium on Advanced Concepts and Techniques in the Study of Snow and Ice Resources*, Monterey, California (H.S. Santeford and J.L. Smith, Eds.), p. 244-254.

Janssen, H.A. (1895) Versuch über Getreidedruck im Silozellen (in German). *V.D.I.*, vol. 38, p. 1045-1049.

Jenike, A.W. (1961) Gravity flow of bulk solids. Utah Engineering Experiment Station Bulletin no. 108.

Jenike (1964) Steady gravity flow of frictional-cohesive solids in converging channels. *Journal of Applied Mechanics*, vol. 31, p. 5-11.

Jenike, A.W. and R.T. Shield (1959) On the plastic flow of Coulomb solids beyond original failure. *Journal of Applied Mechanics*, vol. 81, p. 599-602.

Johanson, J.R. and A.W. Jenike (1967) Stress and velocity fields in the gravity flow of bulk solids. Utah Engineering Experiment Station, Bulletin no. 116.

Lee, C.A. (1963) Hopper design up to date. *Chemical Engineering*, vol. 70, no. 7, p. 75.

Mandl, G. and R.F. Lugue (1970) Fully developed plastic flow of granular materials. *Geotechnique*, vol. 20, no. 3, p. 277-307.

Michel, B. (1968) Thrust exerted by an unconsolidated ice cover on a boom. *Proceedings of the Conference on Ice Pressure*, National Research Council of Canada Technical Manual 92, p. 163-170.

Michel, B. (1971) Winter regime of rivers and lakes. CRREL Monograph III-B1a, p. 83-99, AD 724121.

Morrison, H.L. and O. Richmond (1976) Application of Spencer's ideal soil model to granular material flow. *Journal of Applied Mechanics*, vol. 98, no. 1, p. 49-53.

Pariset, E. and R. Hausser (1961) Formation and evolution of ice covers on rivers. *Transactions of Engineering Institute of Canada*, vol. 5, no. 1, p. 41-49.

Richmond, O. and G.C. Gardner (1962) Limiting spans for arching of bulk material in vertical channels. *Chemical Engineering Science*, vol. 17, p. 1071-1078.

Shapiro, L.H. and J.J. Burns (1975) Satellite observations of sea ice movement in the Bering Strait regions. In *Climate of the Arctic*, University of Alaska, Geophysical Institute.

Spencer, A.J.M. (1964) A theory of kinematics of ideal soils under plain strain conditions. *Journal of Mechanics and Physics of Solids*, vol. 14, p. 337-351.

Walker, D.M. (1966) An approximate theory for pressures and arching in hoppers. *Chemical Engineering Science*, vol. 21, p. 975-997.

☆U.S. GOVERNMENT PRINTING OFFICE: 1977 701-555/144